
Article:
Shaukat, F, Raja, G and Frangi, AF orcid.org/0000-0002-2675-528X (2019) Computer-aided detection of lung nodules: A review. Journal of Medical Imaging, 6 (2). ISSN 2329-4302

https://doi.org/10.1117/1.JMI.6.2.020901

Computer-Aided Detection of Lung Nodules: A Review

Furqan Shaukat,[a,*] Gulistan Raja,[a] Alejandro F. Frangi[b]
[a]Department of Electrical Engineering, University of Engineering & Technology, Taxila 47080, Pakistan.
[b]School of Computing and School of Medicine, University of Leeds Woodhouse Lane, Leeds LS2 9JT,UK.

Abstract. This paper presents an in-depth review and analysis of salient methods for computer-aided detection (CAD) of lung nodules. We evaluate current methods for detecting lung nodules using literature searches with selection criteria based on validation dataset types, nodule sizes, numbers of cases, types of nodules, extracted features in traditional feature-based classifiers, sensitivity, and false positives (FP)/scans. This review shows that current detection systems are often optimized for particular datasets and can detect only one or two types of nodules. We conclude that in addition to achieving high sensitivity and reduced FP/scan, strategies for detecting lung nodules must detect a variety of nodules with high precision to improve on the performances of radiologists. To the best of our knowledge, this is the first review on the effectiveness of feature extraction using traditional feature-based classifiers. Moreover, we discuss deep-learning methods in detail and conclude that features must be appropriately selected to improve the overall accuracy of the system. The aim of this review is to present an analysis of current schemes and highlight constraints and future research areas.

Keywords: computer-aided detection, lung nodule detection, lung cancer, false positive.

1 Introduction

Lung cancer is currently one of the most common causes of death worldwide, with low rates of survival after diagnosis being reported in developed and under-developed countries[1]. According to recent statistics, the 5-year survival rate is only 16%[2] and it has been estimated that by the year 2020, 12 million cancer-related fatalities will occur annually, of which lung cancer will have the largest share[3]. However, survival rates can be improved[1] if nodules are detected early enough. Lung nodules are abnormal growths of tissue that could represent lung cancer. They are typically round/spherical in shape with diameters of up to 30 mm[4]. Nodules are categorized as well-circumscribed, juxta-vascular, juxta-pleural, and pleural-tail. Well-circumscribed nodules are independent and have no extensions into surrounding anatomical structures, whereas juxta-

[*] Corresponding author e-mail address: furqan.shoukat@uettaxila.edu.pk

vascular nodules exhibit strong adherence to proximal vessels, and juxta-pleural nodules are attached to neighboring pleural surfaces. Pleural-tail nodules have tails that are adherent to the nodule but not to pleural walls. Additionally, pulmonary nodules are categorized as solid and subsolid nodules, irrespective of their positions. Subsolid nodules (SSN) are further classified as part-solid nodules and pure ground-glass nodules. Solid nodules are the most common type of nodule, and these repress the underlying functional lung tissues. SSN are pulmonary nodules with partial ground-glass opacity (GGO). These nodules exhibit opacifications with higher density than the surrounding tissues and do not obscure underlying bronchovascular structures[5]. Sample images of different nodules are shown in Fig. 1.

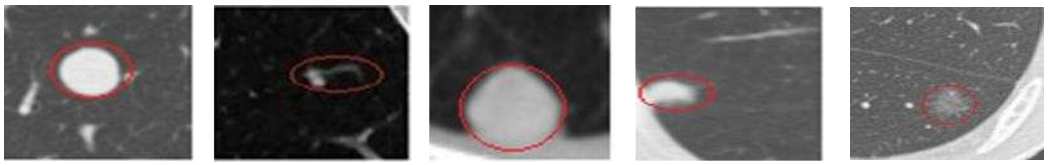

Fig. 1 Samples of lung nodule types. From left to right, well-circumscribed/solid, juxta-vascular/subsolid, juxta-pleural, pleural-tail and GGO nodules

Computer-aided detection (CAD) [6] can assist early diagnosis of lung cancer. The principle aim of CAD is to identify and accurately extract regions of interest (ROI) in images acquired from various imaging modalities, including computed tomography (CT), position emission tomography (PET), and magnetic resonance imaging (MRI) [7–9]. CAD systems can be further categorized as (i) computer-aided detection (CAD_e) and (ii) computer-aided diagnosis (CAD_x). The scope of CAD_e systems is limited to identification of suspicious areas in images, whereas CAD_x systems facilitate disease diagnosis[3]. In the present manuscript, we focus on CAD_e systems. A complete schematic of lung CAD_e processes is shown in Fig. 2.

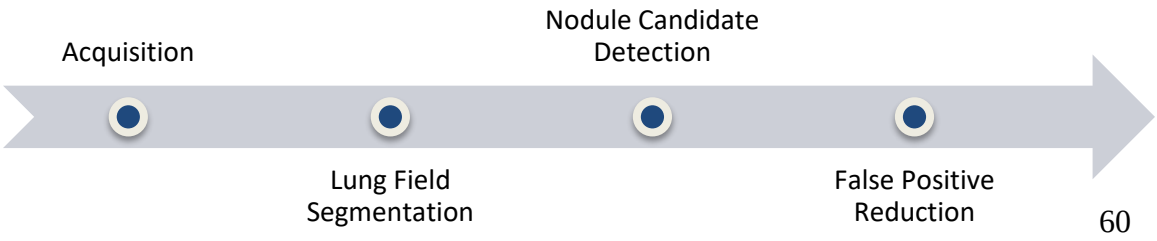

Fig. 2 Typical lung CAD processes: image acquisition, segmentation of lung fields, detection of candiate nodules, and false positive reduction

Medical images are acquired from various imaging modalities[3]. Among these, CT is a fundamental imaging technique for screening analyses of lung nodules, and the other available methods are of less importance. Among public databases, such as the Early Lung Cancer Action Program (ELCAP) Public Lung Image Database[10] and Public Lung Database to Address Drug Response[11], the Lung Image Database Consortium (LIDC)[12] is widely used for its images because they carry standard radiological annotations. The most commonly used public databases are summarized in Table 1.

Table 1. Public Databases for assessments of Lung CAD_e Systems, *N/A, Not available

Database	Release Date	No of Scans	No of images	Modality	Ground truth
VIA/ELCAP [10]	2003	50	N/A	CT	Available
Public Lung Database to Address Drug Response [11]	2005	100	N/A	CT	Available
LIDC-IDRI [12]	2011	1018	244, 527	CT	Available
SPIE-AAPM [13]	2015	70	22489	CT	Available
RIDER Lung PET-CT [14]	2013	275	269, 511	CT, PET	N/A
RIDER Lung CT [15]	2009	46	15,419	CT	Available
QIN Lung CT [16]	2016	47	3954	CT	N/A
Lung CT Segmentation Challenge 2017 [17]	2017	60	9569	CT, RT	N/A
Lung CT-Diagnosis [18]	2015	61	4682	CT	Available (*Tumor Slices*)
ANODE09 [19]	2009	55	N/A	CT	Available (*only for 5 training scans)*

Other platforms that have contributed datasets to the research community include the Dutch–Belgian randomized lung cancer screening trial NELSON[20] and the Lung Cancer Alliance[21]. The main objective of these publicly available databases is to provide data resources to the research community for the development, evaluation, and benchmarking of CAD_e systems.

Lung segmentation is a process by which lung volumes are extracted from CT images and insignificant constituents are discarded. The efficiency of lung nodule detection systems is increased by accurate lung segmentation and several techniques for extracting lung volumes from CT images are used These include, optimal thresholding, rule-based region growing, global thresholding, 3-D-adaptive fuzzy thresholding, hybrid segmentation, and connected component labeling. Following preliminary lung segmentation, juxta-pleural nodules are added by refining extracted lung volumes, generally using a chain-code method, a rolling ball algorithm, or morphological approaches[22–31].

Nodule detection can be described as a process in which suspicious lung areas are detected which may be responsible for lung cancer. Among reported techniques for detecting lung nodules as candidate lung cancers, multiple gray-level thresholding is the most widely considered, although shape-based, template matching-based, morphological approaches with convexity models, and filtering-based methods have also been used for this purpose[22–26,32–33].

Following detection of candidate nodules, nodules must be distinguished from non-nodules. In published studies, this false positive reduction involves feature extraction and nodule classification using feature-based classifiers. Various methods are reported for extracting image features and classifying nodules, generally based on intensity-based statistical features, geometric features, and gradient features[22–23]. After feature extraction, nodule detection is performed using several supervised and unsupervised classifiers to reduce numbers of false positives[24–26, 28, 34–36]. However,

developments in deep-learning have made the selection of image features less explicit, and optimal loss functions and efficient optimization algorithms that influence the learning process have been favored.

In Sec. 2, we present a review of studies that were selected for their relevance to CAD_e. We only considered studies from 2009 because the approaches reported prior to this time have become redundant. Our analyses of these studies are presented with a focus on limitations. Abstracts were retrieved from PubMed, Science Direct, IEEE Xplore, and Web of Science using the keywords "lung," "nodule," "detection," "pulmonary," "tumor," "CAD," "CAD_e," and "cancer" with various combinations of logical expressions containing "AND" and "OR." We reviewed only peer-reviewed archival journal publications and included key conference papers that were published in the last year. Section 3 presents a discussion of the major constraints on present and future prospects. Conclusions are drawn in Sec. 4. The aim of this review was to provide a critical analysis of current lung nodule detection systems and highlight the constraints and future research areas.

2 Review of Lung Nodule Detection Systems

Lung nodule detection systems comprise processes for (i) lung segmentation, (ii) nodule candidate detection, and (iii) false positive reduction. Several reviews of the methods used for nodule detection and false positive reduction identify overall sensitivity and numbers of false positives (FP)/scan as key performance criteria[37–41], but few comparative analyses have been performed to determine the effectiveness of the extracted features that are used for false positive reduction. Therefore, we summarized the techniques for extracting features using feature-based classifiers that are used to determine the most relevant feature classes in lung nodule detection systems and to facilitate sensitivity and reduce FP/scans of the system. Furthermore, we reviewed reports of deep-learning techniques and compared their outcomes with those of traditional feature-based

techniques. To the best of our knowledge, our review is comprehensive and up-to-date and comprises developments in the field. The present review highlights the challenges and constrains of the three categories of lung nodule detection system.

2.1. Lung Segmentation

Lung segmentation techniques can be broadly classified as (i) deformable boundary-based techniques, (ii) edge-based techniques, and (iii) threshold-based techniques. Each lung segmentation technique has its own pros and cons. Although threshold-based techniques are efficacious with high contrast CT images, their performance can vary with low contrast pathologies. Moreover, thresholding can be affected by differing imaging protocols and image acquisition scanners. Particularly, because lung structures, such as blood vessels, bronchioles, and bronchi, exhibit close densities with chest tissues, it is extremely challenging to accurately define ROIs and often requires special post-processing for accurate segmentation. Deformable boundary-based techniques have the disadvantage of extra sensitivity to initialization. Furthermore, they are unable to overcome the heterogeneity of lung volumes with traditional external forces, such as edges and gray levels. Therefore, accurate lung segmentation is difficult using the deformable model. In addition, the accuracy of these imaging analyses depends on the accuracy of registration of prior shape-models for CT images. Poor registration can affect the overall performance and is the main limitation of these schemes. Additionally, the diversity of lung pathologies complicates the accurate segmentation of lung fields. Selected reports of lung segmentation techniques are summarized in Table 2.

2.2. Nodule Candidate Detection

Nodule candidate detection is performed to identify structures within the lung that are suspicious for being lung nodules. This process is typically performed following lung segmentation to decrease the workload

Table 2. Review of Lung Segmentation Techniques[†]

CAD Systems	Year	No. Cases	Image size	Proposed Technique	Ground Truth	Performance
Soliman et al.[50]	2017	105	512 × 512 × 270–450	Shape-based	75 Manual traced scans	OM= 0.98 DSC= 98.4 %
Filho et al.[51]	2017	40 CT scans	512 * 512	Shape-based deformable model	Semi-automatic (manual + commercial software)	FM = 99.14%
Shi et al.[55]	2016	23 CT scans	512 * 512	Thresholding	23 manually traced data	OM= 0.98
Dai et al. [49]	2015	NA	512 * 512* 368	Shape-based	Manually traced data	DSC=0.98
Mansoor et al.[48]	2014	400 CT images	NA	Shape-based	400 manually traced data	OM=0.95
Sun et al.[47]	2012	30 scans	512 × 512 × 424–642, 0.6–0.7 mm thin	Shape-based	30 manually corrected traced data	DSC = 0.97 AD = 0.84 mm
Sofka et al.[46]	2011	260 scans	0.5–5.0 mm	Shape-based	68 manual traced data	SCD = 1.95
Besbes and Paragios[45]	2011	247 image radiographs	256 × 256, 1 mm thin	Shape-based	123 manual traced data	OM = 0.94 AD = 1.39 pixel
Annangi et al.[44]	2010	1130 image radiographs	128 × 128 and 256 × 256	Shape-based deformable model	1130 manually traced images	DSC = 0.88
El-Baz et al.[43]	2008	10 image datasets	512 × 512 × 182, 2.5 mm thin	Statistical MGRF model	1820 manual traced images	Accu. = 0.96

[†] * NA, not available, OM, overlap measure is defined as the volume of the intersection divided by the volume of the union of two samples; DSC, dice similarity coefficient is used to compare the similarity of two samples; FM, F-measure denotes the harmonic mean of predictive value and sensitivity; RmsD, root mean square difference of the distance between the segmentation and the ground truth; SCD, symmetrical point-to-mesh comparison error; AD, mean absolute surface distance is defined as symmetric border positioning measure integrated along entire surfaces.

Shi et al. [42]	2008	247 image radiographs	256 × 256	Shape-based deformable model	247 manual traced images	OM = 0.92 AD = 1.78 pixel
Gao et al.[54]	2007	8 subjects	512 × 512 × 240	thresholding	8 manual traced datasets	DSC = 0.99
Korfiatis et al.[53]	2007	23 scans	512 × 512	Wavelet edge detector	22 manual traced data	OM = 0.98 AD = 0.77 mm
Campadelli et al.[52]	2006	487 image radiographs	256 × 256	Spatial edge detector	487 manual traced data	Sen. = 0.92 Spec. = 0.96
Sluimer et al.[27]	2005	26 scans	512 × 512, 0.75–2.0 mm	Shape-based	10 manual traced Data	OM = 0.82 AD = 1.48 mm

by removing the background and unwanted areas from input CT images. Various methods have been described for detecting lung nodule candidates, and multiple gray-level thresholding is considered the best method, although shape-based, template-matching-based, morphological approaches with convexity models and filtering-based methods have been used.

Akram et al.[56] applied multiple gray level thresholding for nodule candidate detection and stated that single threshold values are insufficient because vessels and different types of nodules exhibit different density values. Choi and Choi[4] reported that nodules exhibit a circular or dot-like shape of variable size. The authors suggested that single-scale enhancement is not appropriate for all nodules and report the use of a multi-scale dot enhancement filter. After enhancement, lung nodules were detected using thresholding. Gonçalves et al.[57] and Chen et al.[58] reported the use of Hessian matrix-based approaches for lung nodule detection. Gonçalves et al.[57] used the central adaptive medialness principle for lung nodule identification and segmentation with shape indices and curvedness properties. They validated their method with 569 solid nodules of the LIDC-IDRI

dataset and demonstrated superior results compared with those obtained via manual segmentation by expert radiologists. Choi and Choi[9] proposed an entropy-based lung nodule detection system involving three stages. In the first stage, CT images are divided into informative and non-informative blocks and the latter are filtered out. In the next step, candidate nodules are detected using informative blocks after enhancement using 3-D coherence-enhancing diffusion. Candidate nodules are then detected from enhanced informative image blocks using optimal thresholding. Finally, certain features are extracted from lung nodule candidates and false positive reduction is performed using a support vector machine (SVM).

In this section, studies are grouped according to the template matching methods for lung nodule candidate detection. Jo et al.[59] proposed lung nodule detection systems using template matching and reported a method based on global rib matching and nodule template matching. In their global rib matching analyses, the lungs were aligned at their centers and rigid registration was performed using coronal and sagittal maximum intensity projection images. In the second step, lung nodule candidates were detected using template-matching-based on density similarities and geometrical correlations between nodules and other neighboring structures. Moreover, El-Baz et al.[60] used 2D and 3D deformable templates and a genetic optimization algorithm to detect lung nodule candidates.

Various morphological approaches have been used to detect lung nodule candidates. Cascio et al.[61] proposed a lung nodule detection method using 3D Mass Spring Model. In their system, region-growing and morphological operations for lung volume segmentation were used, and lung nodule candidates were detected using a 3D mass spring model. The range of gray values and corresponding shape information from the model helped in identifying lung nodule candidates with greater accuracy. The authors validated their system using 84 scans obtained from the LIDC

dataset. Soltaninejad et al.[62] proposed a lung nodule detection scheme using active contours and a KNN classifier. After performing lung volume segmentation using adaptive thresholding and morphological operations, the lung nodule candidates were detected using 2D stochastic features, followed by extraction using active contour modeling. Finally, false positives were reduced using the KNN classifier. Jiantao et al.[32] proposed a shape-based lung nodule detection method comprising the three main steps: modeling, break, and repair. Initially, ROIs were extracted and represented as a shape model using the marching cubes algorithm and the problematic regions were identified and removed using principal curvature analyses, which can lead to inaccurate segmentation of objects. Finally, incomplete regions were fitted using interpolation and extrapolation with a radial basis function for smoothly estimating and repairing suspicious areas. Kubota et al.[33] proposed a lung nodule detection method using morphological operations and convexity models. Initially, lung volumes were extracted using voxel transformation and figure ground separation. Subsequently, a Euclidian distance map was used to locate the seed point and then region growing was applied to identify candidate nodule regions. Finally, the authors segmented candidate lung nodules using convex hull. Reported techniques for lung nodule detection are summarized in Table 3.

Table 3. Review of Lung Nodule Detection Methods

CAD Systems	Year	Detection Technique
Akram et al.[56],	2016	Multiple gray-level thresholding
Choi and Choi [4]	2014	Multi-Scale Dot Enhancement Filter
Gonçalves et al.[57], Chen et al.[58]	2016, 2012	Hessian Matrix-Based Method
Choi and Choi [9]	2013	Entropy Analysis

Jo et al. [59]	2014	Template Matching
El-Baz et al.[60]	2013	Template Matching and Genetic Algorithm
Cascio et al.[61]	2012	Stable 3D Mass Spring Models
Soltaninejad et al.[62]	2012	Active Contour and K-Nearest Neighbors (K-NN) Classifier
Jiantao et al.[32]	2011	Thresholding and Geometric Modeling
Kubota et al.[33]	2011	Convexity model and Morphological Approach
Riccardi et al.[63]	2011	3D Fast Radial Transform
Namin et al.[64] **and Murphy et al.**[65]	2010, 2007	Shape Index
Ozekes et al.[66]	2008	3D Template Matching

In summary, the most commonly used lung nodule detection techniques can be broadly classified into the three main categories (i) thresholding, (ii) template matching, and (iii) morphological approaches. Thresholding based results depend on the qualities of techniques for threshold adjustment. Template-matching techniques suffer from irregular shapes and diversities of lung nodule types. Template-matching methods also generally assume that nodules are spherical or cylindrical, and are hence, challenged by nodules that are attached to the pleura and vessels. Alternatively, morphological approaches suffer from low detection efficiency for lung wall nodules.

2.3. False Positive Reduction

After detecting nodule candidates, they are classified into nodules and non-nodules. This step is commonly referred to as false positive reduction and is performed using the following two broad categories of methods: (i) conventional feature-based classifiers and (ii) convolutional neural

networks. Conventional feature-based classification is performed using (i) feature extraction and (ii) nodule candidate classification techniques. Several methods for feature extraction and nodule candidate classification have been proposed. Below, we briefly review published studies in both of these categories and highlight the challenges inherent in the respective CAD systems.

In 2009, Cuenca et al.[25] proposed a CAD system using an iris filter to detect isolated pulmonary nodules from CT images. The system achieved a sensitivity of 80% with 7.7 FP/scan. The system could only detect one type of nodule, although the used dataset was quite small and contained only 77 nodules. In contrast, Murphy et al.[67] used a large private dataset of 813 scans for the evaluation of their proposed system and achieved a sensitivity of 80% with 4.2 FP/scan. They used local image features and the k-nearest-neighbor classification. Despite their large dataset, the sensitivity of their system was lower than that of other reported systems. Similarly, Guo et al.[68], Liu et al.[69], Retico et al.[70], and Messay et al.[22] used small datasets comprising 29 scans (34 true nodules), 32 scans (33 solitary nodules), 42 scans (102 pleural nodules), and 84 scans (150 nodules), respectively, for evaluation of their proposed systems. It is presumed that the performances of these systems will be poor in realistic scenarios with a broader range of nodule types seen in clinical scans.

In 2010, S. Ozekes et al.[71] proposed a computerized lung nodule detection method using 3D feature extraction and learning-based algorithms. They claimed a sensitivity of up to 100%, but a false positive rate of 44 per scan rendered the method inefficient. An automatic CAD system was proposed by Sousa et al.[72], which used an optimized subset of eight features from a total of 24 initially extracted features. The system achieved a false positive rate of 0.42 and a sensitivity of 84.84%. However, it was tested with only 33 nodules, making its performance susceptible to differing scenarios. In 2012, Mabrouk et al.[7] proposed a technique for automatically detecting lung

nodules from CT images using two classifiers. A total of 22 image features were extracted for their model and feature selection was driven by Fisher scores. Although the system exhibited good performance with respect to detection of large nodules, it was not able to detect smaller nodules.

In 2013, Assefa et al.[73] proposed a nodule detection scheme based on template matching and multi-resolution based false reduction. Seven statistical and two intensity-based features were extracted for the false positive reduction stage and the system performed at an 81% classification rate. However, this system also had a very high false positive rate (35.15%), leading to disadvantages in terms of inefficiency. Choi et al.[9] proposed a method based on hierarchical block classification in which sub-blocks of the image were constructed and entropy-based analysis was then used to select those with high entropy. The proposed system achieved a sensitivity of 95.28% with only 2.27 FP/scans. This system had good overall performance but failed to detect all types of nodules. Tariq et al.[74] proposed a computerized system for lung nodule detection from CT scan images using a neuro-fuzzy classifier; however, no standard datasets or performance metrics were used to evaluate its performance. Orozco et al.[75] extracted eight texture features from histograms and a gray-level co-occurrence matrix, which were given as input to SVM for false positive reduction. The system achieved a reliability index of 84% but was evaluated using a private dataset of only 38 scans with nodules. Tartar et al.[76] detected pulmonary nodules using hybrid features: a total of 30 intensity-based and geometrical (2D & 3D) features were extracted and given as input to four different classifiers. Their system achieved a sensitivity of 89.6% but was evaluated using a private dataset comprising only 95 pulmonary nodules.

In 2014, Teramoto et al.[77] proposed a hybrid method for detecting pulmonary nodules using PET/CT. They used 100 PET/CT images to evaluate their method, which achieved a sensitivity of 83.0% with 5 FP/scan. Although their system relied on a novel combination of CT/PET images, it

did not achieve high sensitivity. Choi et al.[4] introduced a 3D shape-based feature descriptor to detect pulmonary nodules in CT images. The system was evaluated using the LIDC dataset with 148 nodules and achieved a sensitivity of 97.5% with 6.76 FP/scan. Although it showed good performance overall, the FP/scan was unfavorable. In 2016, Akram et al.[56] reported a SVM-based classification of lung nodules using hybrid features from CT images. Similar to other studies, their system was validated with insufficient nodules to achieve the same performance under various scenarios. Other selected studies[78-81] that used conventional feature-based classification are summarized in Table 4.

This section presents selected studies that used convolutional neural networks (CNN) for pulmonary nodule detection. In 2015, Setio et al.[82] proposed a multi-view convolutional network-based lung nodule detection system with three dedicated detectors for large, subsolid, and solid nodules. The final detection step was performed using multiple streams of 2D convolutional networks and a dedicated fusion method. This system was evaluated using 888 scans from the LIDC-IDRI dataset and achieved a detection sensitivity of 90.1% with only 4 FP/scans. Anirudh et al.[83] used a 3D CNN to learn discriminative features for nodule detection. The proposed system was evaluated using 67 scans from the SPIE-LUNGx dataset and achieved a relatively lower sensitivity of 80% with 10 FP/scan. In 2017, Ding et al.[84] proposed a lung nodule detection system based on deep CNNs. Their system involved the application of a region-based CNN for nodule detection on image slices and employed a 3D CNN to reduce false positives. It was evaluated using the Lung Nodule Analysis Challenge (LUNA16) dataset and achieved a high sensitivity (94.4%) with only 4 FP/scan. Zhu et al.[85] developed the automatic lung nodule detection and classification system DeepLung, which included nodule detection and classification. Nodule detection was

achieved using a 3D Fast regional CNN (R-CNN) and the system achieved a relatively lower detection sensitivity of 83.4%.

In 2018, Gruetzemacher et al.[86] proposed a novel lung nodule detection method using two 3D CNNs: the first was used to generate candidate nodules and the second was used to reduce false positives. Using 888 scans from the LIDC dataset, a sensitivity of 89.29% was demonstrated with 1.78 FP/scan. Xie et al.[87] proposed a lung nodule detection method that employed different approaches for feature extraction. Feature representations of nodules were learned using deep CNN and candidate nodules were classified as nodules or non-nodules using the AdaBoost back propagation neural network. The proposed system achieved a sensitivity of 84.19% with 7.98 FP/scan. Similarly, Kim et al.[88] proposed a lung nodule detection method using multi-scale gradual integration of CNN in a three-step method. Multi-scale patches with differing levels of contextual information were gradually integrated using zoom-in and zoom-out streams. The reported CPM of 0.942 indicates an average sensitivity of analyses performed at 7 different false positive rates using the LIDC dataset for evaluation. In their CAD system, Qin et al.[89] used a 3D CNN model that employed 3D U-Net architecture as the backbone for a region proposal network (RPN). It had a sensitivity of 98.2% with only 4 FP/scan. In 2019, Xie et al.[90] contributed a 2D CNN for pulmonary nodule detection. They detected nodule candidates by adjusting the structures of a Faster R-CNN with two RPNs and a deconvolution layer. Their approach was extensively evaluated using the LIDC dataset used in the LUNA16 study and achieved a sensitivity of 86.4% with only 4 FP/scan. The CAD systems described above are summarized in Table 4.

Table 4. Performance Comparison of Different CAD Systems; *N/A, Not available.

CAD Systems	Data Set	No. Cases	No. Nodules	Nodule Size (mm)	Extracted Features	Sensitivity (%)	FPR	Type of Nodules	Remarks
Guo *et al.*[68]	Private	29	34	N/A	Shape	94.77	N/A	N/A	
Sousa *et al.*[72]	Private	N/A	33	3–40	Shape, Texture, Gradient, Histogram, Spatial	84.84	0.42	Isolated, Juxta-pleural and Juxta-vascular	Used dataset is too small containing less number of nodules.
Liu *et al.*[69]	Private	32	33	3–17	N/A	93.75	4.60	Juxta-pleural	
Orozco *et al.*[75]	LIDC, ELCAP	128	75	2–30	Texture	84.00	7.00	N/A	
Tartar *et al.*[76]	Private	63	95	2–20	Shape	89.60	7.90	Well-circumscribed, Vascularized, Juxta-pleural, Pleural-tail	
Messay *et al.*[22]	LIDC	84	143	3–30	Shape, Intensity, Gradient.	82.66	3.00	Juxta-vascular and Juxta-pleural	Systems underperform in terms of sensitivity/ accuracy.
Murphy *et al.*[67]	Private	813	1518	2–14	Shape Index, Curvedness	80.00	4.20	Non-solid, Part-Solid, Solid	
Retico et *al.*[70]	Private	42	102	6–30	Morphological, Texture	72.00	6.00	Pleural	
Teramoto *et al.*[77]	Private	100	103	4–30	Shape, Intensity	83.00	5.00	Solitary	
Gong et al.[80]	LIDC	888	1186	3–30	Intensity, Shape, Texture	79.30	4.00	Solid and GGO	
Bergtholdt et al.[91]	LIDC	243	690	3–30	Shape, Intensity, Gradient.	85.90	2.50	Juxta-pleural	
Opfer *et al.*[92]	LIDC	91	N/A	3–30	Shape, Intensity	78.00	2.00	N/A	
Sahiner *et al.*[93]	Private, LIDC	85	241	3–19	Shape, Statistical, Gradient	76.00	5.60	N/A	

Suzuki *et al.*[94]	Private	63	121	4–27	N/A	80.30	4.80	Pure GGO, Mixed GGO and Solid	
Ozekes *et al.*[71]	LIDC	11	11	3–16	Shape	100.00	44.00	Solitary	High false positive rate
Assefa *et al.*[73]	ELCAP	50	165	N/A	Intensity, Statistical	81.00	35.15	N/A	makes the schemes inefficient.
Torres et al. [95]	LIDC	949	1749	3–30	Shape, Intensity	80.00	8.00	GGO	
Choi et al. [4]	LIDC	84	148	3–30	Shape-Based 3D Descriptor	97.50	6.76	Solid, Juxta-pleural	
Mabrouk *et al.*[7]	Private	12	N/A	22–42	Shape, Intensity	97.00	2.00	N/A	System's ability to detect all type of nodules is limited.
Choi *et al.*[9]	LIDC	58	151	3–30	Shape, Intensity	95.28	2.27	Juxta-pleural	
Akram *et al.*[56]	LIDC	47	50	3–30	Shape, Intensity	95.31	N/A	Juxta-pleural	System is evaluated with small number of nodules and FP/scan is not informed
Wang et al.[81]	LIDC	1010	673	3–30	CS-LBP and ORT-EOH	95.69	3.05	Solid, GGO, Juxta-vascular and Juxta-pleural	
Setio et al.[82]	LIDC	888	1186	3–30	Convolutional Neural Network	90.10	4.00	Solid, Subsolid, Juxta-pleural	Developments on deep-learning have made less explicit the selection of the image features, which has
Anirudh et al.[83]	SPIE-AAPM LUNG	67	N/A	3–30	Convolutional Neural Network	80.00	10.00	Solid, Part-solid and Non-solid	
Ding et al.[84]	LIDC	888	1186	3–30	Convolutional Neural Network	94.40	4.00	N/A	
Gruetzemacher et al.[86]	LIDC	888	1186	3–30	Convolutional Neural Network	89.29	1.79	Juxta-pleural and Juxta-vascular	
Xie et al.[87]	LIDC	1018	2669	3–30	Convolutional	84.19	N/A	N/A	

					Neural Network				now turned to select optimal loss functions and efficient optimization algorithms influencing the learning process. Besides, CNN may have a high computational cost and requires a large dataset for training.
Kim et al.[88]	LIDC	888	1166	3–30	Convolutional Neural Network	95.20	2.00	N/A	
Qin et al.[89]	LIDC	888	1186	3–30	Convolutional Neural Network	98.2	4.00	N/A	
Xie et al.[90]	LIDC	1018	N/A	3–30	Convolutional Neural Network	83.2	4.00	Solitary, Vascularized, Juxta-pleural and Pleural-tail	
Dou et al.[96]	LIDC	888	1186	3–30	Convolutional Neural Network	90.70	4.00	Solitary, GGO Pleural	
Jiang et al.[97]	LIDC	1006	2669	3–30	Convolutional Neural Network	80.06	4.70	Juxta-pleural nodule	
Jin et al.[98]	LIDC	888	1186	3–30	Convolutional Neural Network	92.40	2.00	Solid, Subsolid, Pleural	
Dou et al.[99]	LIDC	888	1186	3–30	Convolutional Neural Network	90.60	2.00	N/A	

3. Discussion

To identify challenges and future research directions, we summarized selected lung nodule detection systems reported in the literature since 2009. In this review of current methods, direct comparisons of research results were hampered by diverse performance metrics and evaluation protocols. Nonetheless, we evaluated the present systems according to datasets used, number of subjects considered, nodule sizes, nodule numbers, and the standard performance metrics

sensitivity and FP/scan. We also compared lung nodule features that were extracted in the reviewed studies, and identified the most relevant features for effective lung nodule detection systems. To this end, we grouped reported systems into the following categories:

i. Papers with small datasets and small numbers of nodules; the performance of these systems will likely deteriorate under more realistic scenarios with more various nodule types, as present in clinical scans.

ii. Papers reporting systems with poor accuracy/sensitivity compared with other systems;

iii. Papers in which high false positive rates hamper efficiency

[91–99] were included in the table based on relevance, and the results of some other studies [100–102] were omitted due to the absence of relevant information. Collectively, the studies included in Table 4 indicate that the major challenge for lung nodule detection systems is robustness to diverse clinical data of varying quality. In particular, most algorithms were optimized using private datasets, thus limiting comparability and generalization of the results. In addition, to ensure robustness, the proposed methods need to be validated with sufficiently large datasets that include all nodule types. Accordingly, methods that were evaluated with fewer nodules will likely lose accuracy under clinical conditions in which, nodule types are more varied. Feature extraction serves as an important step in differentiating nodules from other anatomic structures present in lung lobes. Yet, optimal set of features for nodule detection remain a subject of debate. The major constraints of lung nodule detection are summarized as follows:

i. Nodule detection methods are demonstrated using particular datasets.

ii. Few methods have been validated with large datasets.

iii. Optimal selection of features for nodule detection.

iv. Robustness to diverse nodule types.

v. Inconsistent use of performance metrics.

vi. Robustness to diverse lung nodule size.

Constraints that influence nodule detection remain a challenge in this area, in part because reported systems have been developed to accommodate the specific requirements of the investigating practitioners. The remaining challenge is to develop more accurate and robust systems that identify a broad range of nodules with increased sensitivity and reduced FP/scan. Some of the present studies, however, have the potential to facilitate the development lung cancer diagnosis tools. Specifically Choi et al.[4], El-Baz et al.[43], Mansoor et al.[48], Dai et al.[49], Soliman et al.[50], Filho et al.[51], Setio et al.[82], Ding et al.[84] and Shaukat et al.[78] achieved high performance metrics and validated their methods using large public datasets, such as the LIDC[12]. This database is distinguished by standard radiological annotations that were generated by four expert radiologists in two consecutive sessions.

3.1 Future Prospects

Much further research is required to improve CAD systems for lung cancer. Despite the considerable volume of research in this area, no commercial products are available for use in hospitals, reflecting the need for further research and development of the related technologies. The following critical topics can be identified in collective considerations of the present reviewed studies:

1. Segmentation of suspected pulmonary nodules requires further research and development. Accurate pulmonary nodule segmentation can increase the detection sensitivity of CAD systems.

2. CAD systems need to be validated with sufficiently large datasets to demonstrate robustness. Many CAD systems have only been evaluated on relatively small datasets, and their performance

will likely be reduced in real clinical scenarios. More extensive experiments will provide assessments of the generalizability and clinical performance of these detection systems.

3. Selection of optimal features for lung nodule detection is another area needing further investigation. Although deep-learning technologies avoid handcrafting and selecting image features, they instead require selection of a loss function, network architecture, and an efficient optimization method, all of which influence the learning process.

4. Future CAD systems should be able to detect all types of nodules with the same precision and sensitivity and with reduced FPs/scan.

4. Conclusion

The existing methods for detecting lung nodules need to be improved, and this may be achieved by proposing new techniques and providing novel solutions. Future CAD_e systems will be expected to detect all types of nodules with high precision and sensitivity, and with few false positives per scan. To ensure robustness, proposed systems will need to be evaluated on large datasets so that evaluations of multiple datasets with standard performance metrics can be performed with accuracy. A well performing CAD system would save many lives by facilitating early detection of lung nodules and providing a second opinion to that of expert radiologists.

Disclosures

The authors declare no conflicts of interest.

Acknowledgments

The authors would like to thank Enago (www.enago.com) for the English language review.

References

1. R. Siegel, K. Miller, and A. Jemal, "Cancer statistics, 2018.," CA Cancer J Clin **68**(1), 7–30 (2018).
2. P. Bach, et al., Benefits and harms of CT screening for lung cancer," JAMA **307**(22), 2418–2429 (2012).
3. D. Forman et al. "The global and regional burden of cancer." World Cancer Report 2014, 16–53 (2014).
4. W.J. Choi and T.S. Choi, "Automated pulmonary nodule detection based on three-dimensional shape-based feature descriptor," Comput. Methods Programs Biomed. 113(1), 37–54 (2014).
5. H. MacMahon, et al., "Guidelines for Management of Incidental Pulmonary Nodules Detected on CT Images: From the Fleischner Society 2017," Radiology **284**(1), 228–243 (2017).
6. S.S. Parveen and C. Kavitha, "A Review on Computer Aided Detection and Diagnosis of lung cancer nodules," Int. J. Comput. Technol. **3**(3), 393–400 (2012).
7. M. Mabrouk, A. Karrar, and A. Sharawy, "Computer Aided Detection of Large Lung Nodules using Chest Computer Tomography Images," Computer (Long. Beach. Calif). **3**(9), 12–18 (2012).
8. S.K. Vijai Anand, "Segmentation coupled textural feature classification for lung tumor prediction," in 2010 Int. Conf. Commun. Control Comput. Technol.(IEEE, 2010), pp. 518–524.
9. W.J. Choi and T.S. Choi, "Automated pulmonary nodule detection system in computed tomography images: A hierarchical block classification approach," Entropy **15**(2), 507–523 (2013).
10. C.I. Henschke, et al., "Early lung cancer action project: a summary of the findings on baseline screening.," Oncologist **6**(2), 147–52 (2001).
11. "Public Lung Image database to address drug response. Vision and Image Analysis Group (VIA) and International Early Lung Cancer Action Program (I-ELCAP) Labs, Cornell University." (accessed 24-04-16). [http://www.via.cornell.edu/crpf.html; 2008]

12. S.G. Armato, et al., “The Lung Image Database Consortium (LIDC) and Image Database Resource Initiative (IDRI): a completed reference database of lung nodules on CT scans.,” Med. Phys. **38**(2), 915–931 (2011).
13. S.G. Armato et al., “Guest Editorial: LUNGx Challenge for computerized lung nodule classification: reflections and lessons learned,” J. Med. Imaging **2**(2), 020103 (2015).
14. P. Muzi et al., “Data From RIDER Lung PET-CT. The Cancer Imaging Archive.,” (2015) [http://doi.org/10.7937/K9/TCIA.2015.OFIP7TVM]
15. B. Zhao et al., “Evaluating Variability in Tumor Measurements from Same-day Repeat CT Scans of Patients with Non–Small Cell Lung Cancer,” Radiology **252**(1), 263–272 (2009).
16. J. Kalpathy-Cramer et al., “A Comparison of Lung Nodule Segmentation Algorithms: Methods and Results from a Multi-institutional Study,” J. Digit. Imaging **29**(4), 476–487 (2016).
17. J.S. Yang et al., “Data from Lung CT Segmentation Challenge. The Cancer Imaging Archive.,” (2017) [http://doi.org/10.7937/K9/TCIA.2017.3r3fvz08]
18. O. Grove et al., “Quantitative Computed Tomographic Descriptors Associate Tumor Shape Complexity and Intratumor Heterogeneity with Prognosis in Lung Adenocarcinoma,” PLoS One **10**(3), e0118261 (2015).
19. B. van Ginneken et al., “Comparing and combining algorithms for computer-aided detection of pulmonary nodules in computed tomography scans: The ANODE09 study,” Med. Image Anal. **14**(6), 707–722 (2010).
20. Y. Ru Zhao, et al., “NELSON lung cancer screening study.,” Cancer Imaging **11**(1A), S79–84 (2011).
21. “Lung Cancer Alliance,” (accessed 13-04-18) [https://lungcanceralliance.org]
22. T. Messay, R.C. Hardie, and S.K. Rogers, “A new computationally efficient CAD system for pulmonary nodule detection in CT imagery,” Med. Image Anal. **14**(3), 390–406 (2010).

23. W.J. Choi and T.S. Choi, “Genetic programming-based feature transform and classification for the automatic detection of pulmonary nodules on computed tomography images,” Inf. Sci. (Ny). **212**, 57–78 (2012).

24. J. Dehmeshki, et al., “Automated detection of lung nodules in CT images using shape-based genetic algorithm,” Comput. Med. Imaging Graph. **31**(6), 408–417 (2007).

25. J.J. Suárez-Cuenca, et al., “Application of the iris filter for automatic detection of pulmonary nodules on computed tomography images,” Comput. Biol. Med. **39**(10), 921–933 (2009).

26. X. Ye, et al., “Shape based computer-aided detection of lung nodules in thoracic CT images,” IEEE Trans. Biomed. Eng. **56**(7), 1810–1820 (2009).

27. I. Sluimer, M. Prokop, and B. van Ginneken, “Toward automated segmentation of the pathological lung in CT,” Med. Imaging, IEEE. **24**(8), 1025–1038 (2005).

28. G. De Nunzio, et al., “Automatic lung segmentation in CT images with accurate handling of the hilar region,” J. Digit. Imaging **24**(1), 11–27 (2011).

29. A.M. Ali and A.A. Farag, “Automatic Lung Segmentation of Volumetric Low-Dose CT Scans Using Graph Cuts,” in Adv. Vis. Comput. Pt I, Proc.(Springer Berlin Heidelberg, 2008), pp. 258–267.

30. E. van Rikxoort, B. de Hoop, and M. Viergever, “Automatic lung segmentation from thoracic computed tomography scans using a hybrid approach with error detection,” Med. Phys. **36**(7), 2934 (2009).

31. D.S. Paik, et al., “Surface normal overlap: a computer-aided detection algorithm with application to colonic polyps and lung nodules in helical CT,” Med. Imaging IEEE Trans. **23**(6), 661–675 (2004).

32. J. Jiantao Pu, et al., “Shape ‘break-and-repair’ strategy and its application to automated medical image segmentation.,” IEEE Trans. Vis. Comput. Graph. **17**(1), 115–24 (2011).

33. T. Kubota, et al., “Segmentation of pulmonary nodules of various densities with morphological approaches and convexity models,” Med. Image Anal. **15**(1), 133–154 (2011).

34. S.L.A. Lee, A.Z. Kouzani, and E.J. Hu, “Random forest based lung nodule classification aided by clustering,” Comput. Med. Imaging Graph. **34**(7), 535–542 (2010).

35. M. Niemeijer, et al., “On Combining Computer-Aided Detection Systems,” IEEE Trans. Med. Imaging **30**(2), 215–223 (2011).

36. P.G. Espejo, S. Ventura, and F. Herrera, “A Survey on the Application of Genetic Programming to Classification,” IEEE Trans. Syst. Man, Cybern. Part C Appl. Rev **40**(2), 121–144 (2010).

37. S.L.A. Lee, A.Z. Kouzani, and E.J. Hu, “Automated detection of lung nodules in computed tomography images: A review,” Mach. Vis. Appl. **23**(1), 151–163 (2012).

38. K. Suzuki, “A review of computer-aided diagnosis in thoracic and colonic imaging.,” Quant. Imaging Med. Surg. **2**(3), 163–76 (2012).

39. L.H. Eadie, P. Taylor, and A.P. Gibson, “A systematic review of computer-assisted diagnosis in diagnostic cancer imaging,” Eur. J. Radiol. **81**(1), e70–e76 (2012).

40. A. El-Baz et al., “Computer-aided diagnosis systems for lung cancer: challenges and methodologies.,” Int. J. Biomed. Imaging 2013, 942353 (2013).

41. M. Firmino, A.H. Morais, R.M. Mendoça, M.R. Dantas, H.R. Hekis, and R. Valentim, “Computer-aided detection system for lung cancer in computed tomography scans: review and future prospects.,” Biomed. Eng. Online 13, 41 (2014).

42. Yonghong Shi et al., “Segmenting Lung Fields in Serial Chest Radiographs Using Both Population-Based and Patient-Specific Shape Statistics,” IEEE Trans. Med. Imaging **27**(4), 481–494 (2008).

43. A. El-Baz, et al., “A New Stochastic Framework for Accurate Lung Segmentation,” in (Springer, Berlin, Heidelberg, 2008), pp. 322–330.

44. P. Annangi, et al, “A region based active contour method for x-ray lung segmentation using prior shape and low level features,” in 2010 IEEE Int. Symp. Biomed. Imaging From Nano to Macro (IEEE, 2010), pp. 892–895.

45. A. Besbes and N. Paragios, “Landmark-based segmentation of lungs while handling partial correspondences using sparse graph-based priors,” in 2011 IEEE Int. Symp. Biomed. Imaging From Nano to Macro (IEEE, 2011), pp. 989–995.

46. M. Sofka, et al., “Multi-stage learning for robust lung segmentation in challenging CT volumes,” in Proceedings of the International Conference on Medical 27 Imaging Computing and Computer-Assisted Intervention (MICCAI ’11), 2011, pp. 667–674.
47. Shanhui Sun, C. Bauer, and R. Beichel, “Automated 3-D Segmentation of Lungs With Lung Cancer in CT Data Using a Novel Robust Active Shape Model Approach,” IEEE Trans. Med. Imaging **31**(2), 449–460 (2012).
48. A. Mansoor et al., “A Generic Approach to Pathological Lung Segmentation,” IEEE Trans. Med. Imaging **33**(12), 2293–2310 (2014).
49. S. Dai, K. Lu, J. Dong, Y. Zhang, and Y. Chen, “A novel approach of lung segmentation on chest CT images using graph cuts,” Neurocomputing **168**, 799–807 (2015).
50. A. Soliman et al., “Accurate Lungs Segmentation on CT Chest Images by Adaptive Appearance-Guided Shape Modeling,” IEEE Trans. Med. Imaging **36**(1), 263–276 (2017).
51. P.P. Rebouças Filho, et al., “Novel and powerful 3D adaptive crisp active contour method applied in the segmentation of CT lung images,” Med. Image Anal. **35**, 503–516 (2017).
52. P. Campadelli, E. Casiraghi, and D. Artioli, “A Fully Automated Method for Lung Nodule Detection From Postero-Anterior Chest Radiographs,” IEEE Trans. Med. Imaging **25**(12), 1588–1603 (2006).
53. P. Korfiatis, et al., “Combining 2D wavelet edge highlighting and 3D thresholding for lung segmentation in thin-slice CT,” Br. J. Radiol. **80**(960), 996–1004 (2007).
54. Q. Gao, et al., “Accurate Lung Segmentation For X-ray CT Images,” in Third Int. Conf. Nat. Comput. (ICNC 2007)(IEEE, 2007), pp. 275–279.
55. Z. Shi et al., “Many Is Better Than One: An Integration of Multiple Simple Strategies for Accurate Lung Segmentation in CT Images,” Biomed Res. Int. 2016, 1–13 (2016).
56. S. Akram, M.Y. Javed, M.U. Akram, U. Qamar, and A. Hassan, “Pulmonary Nodules Detection and Classification Using Hybrid Features from Computerized Tomographic Images,” J. Med. Imaging Heal. Informatics **6**(1), 252–259 (2016).

57. L. Gonçalves, J. Novo, and A. Campilho, "Hessian based approaches for 3D lung nodule segmentation," Expert Syst. Appl. **61**, 1–15 (2016).

58. B. Chen et al., "Automatic segmentation of pulmonary blood vessels and nodules based on local intensity structure analysis and surface propagation in 3D chest CT images," Int. J. Comput. Assist. Radiol. Surg. **7**(3), 465–482 (2012).

59. H.H. Jo, H. Hong, and J. Mo Goo, "Pulmonary nodule registration in serial CT scans using global rib matching and nodule template matching," Comput. Biol. Med. **45**, 87–97 (2014)

60. A. El-Baz, et al., "Automatic Detection of 2D and 3D Lung Nodules in Chest Spiral CT Scans.," Int. J. Biomed. Imaging 2013, 517632 (2013).

61. D. Cascio, et al., "Automatic detection of lung nodules in CT datasets based on stable 3D mass-spring models," Comput. Biol. Med. **42**(11), 1098–1109 (2012).

62. S. Soltaninejad, M. Keshani, and F. Tajeripour, "Lung nodule detection by KNN classifier and active contour modelling and 3D visualization," 16th CSI Int. Symp. Artif. Intell. Signal Process. (AISP 2012) (Aisp), 440–445 (2012).

63. A. Riccardi, et al., "Computer-aided detection of lung nodules via 3D fast radial transform, scale space representation, and Zernike MIP classification," Med. Phys. **38**(4), 1962–1971 (2011).

64. S. Taghavi Namin, et al., "Automated detection and classification of pulmonary nodules in 3D thoracic CT images," 2010 IEEE Int. Conf. Syst. Man Cybern. 3774–3779 (2010).

65. K. Murphy, et al., "Automated detection of pulmonary nodules from low-dose computed tomography scans using a two-stage classification system based on local image features," in edited by M.L. Giger and N. Karssemeijer (International Society for Optics and Photonics, 2007), p. 651410.

66. S. Ozekes, O. Osman, and O.N. Ucan, "Nodule detection in a lung region that's segmented with using genetic cellular neural networks and 3D template matching with fuzzy rule based thresholding," Korean J. Radiol. **9**(1), 1–9 (2008).

67. K. Murphy, et al., “A large-scale evaluation of automatic pulmonary nodule detection in chest CT using local image features and k-nearest-neighbour classification,” Med. Image Anal. **13**(5), 757–770 (2009).
68. W. Guo, et al., “An adaptive lung nodule detection algorithm,” Chinese Control Decis. Conf., IEEE, 2361–2365 (2009).
69. Y. Liu, et al., “Computer aided detection of lung nodules based on voxel analysis utilizing support vector machines,” FBIE 2009 - 2009 Int. Conf. Futur. Biomed. Inf. Eng. 90–93 (2009).
70. A. Retico, et al., “Pleural nodule identification in low-dose and thin-slice lung computed tomography,” Comput. Biol. Med. **39**(12), 1137–1144 (2009).
71. S. Ozekes and O. Osman, “Computerized lung nodule detection using 3D Feature extraction and learning based algorithms,” J. Med. Syst. **34**(2), 185–194 (2010).
72. J.R.F.D.S. Sousa, et al., “Methodology for automatic detection of lung nodules in computerized tomography images.,” Comput. Methods Programs Biomed. **98**(1), 1–14 (2010).
73. M. Assefa, et al., “Lung nodule detection using multi-resolution analysis,” 2013 ICME Int. Conf. Complex Med. Eng. 457–461 (2013).
74. A. Tariq, M.U. Akram, and M.Y. Javed, “Lung nodule detection in CT images using neuro fuzzy classifier,” 2013 Fourth Int. Work. Comput. Intell. Med. Imaging 49–53 (2013).
75. H.M. Orozco, et al., “Lung Nodule Classification in CT Thorax Images Using Support Vector Machines,” 2013 12th Mex. Int. Conf. Artif. Intell. 277–283 (2013).
76. A. Tartar, N. Kilic, and A. Akan, “Classification of pulmonary nodules by using hybrid features,” Comput. Math. Methods Med. 2013, 1–11 (2013).
77. A. Teramoto, et al., “Hybrid method for the detection of pulmonary nodules using positron emission tomography/computed tomography: A preliminary study,” Int. J. Comput. Assist. Radiol. Surg. **9**(1), 59–69 (2014).
78. F. Shaukat, et al., “Fully automatic detection of lung nodules in CT images using a hybrid feature set,” Med. Phys. **44**(7), 3615–3629 (2017).

79. F. Shaukat, et al., Artificial neural network based classification of lung nodules in CT images using intensity, shape and texture features, J. Ambient Intell. Humaniz. Comput. 1–15 (2019).
80. J. Gong, et al., "Automatic detection of pulmonary nodules in CT images by incorporating 3D tensor filtering with local image feature analysis," Phys. Medica 46, 124–133 (2018).
81. B. Wang, et al., False positive reduction in pulmonary nodule classification using 3D texture and edge feature in CT images, Technol. Heal. Care Preprint(Preprint), 1–18 (2019).
82. A.A.A. Setio, et al., "Pulmonary Nodule Detection in CT Images: False Positive Reduction Using Multi-View Convolutional Networks," IEEE Trans. Med. Imaging **35**(5), 1160–1169 (2016).
83. R. Anirudh, et al., "Lung nodule detection using 3D convolutional neural networks trained on weakly labeled data," in edited by G.D. Tourassi and S.G. Armato (International Society for Optics and Photonics, 2016), p. 978532.
84. J. Ding, et al., "Accurate Pulmonary Nodule Detection in Computed Tomography Images Using Deep Convolutional Neural Networks," in Medical Image Computing and Computer-Assisted Intervention − *MICCAI 2017* (Springer, Cham, 2017), pp. 559–567.
85. W. Zhu, et al., "DeepLung: 3D Deep Convolutional Nets for Automated Pulmonary Nodule Detection and Classification," arXiv preprint arXiv:1709.05538, (2017).
86. R. Gruetzemacher, A. Gupta, and D. Paradice, "3D deep learning for detecting pulmonary nodules in CT scans," J. Am. Med. Informatics Assoc. **25**(10), 1301–1310 (2018).
87. Y. Xie, et al., "Fusing texture, shape and deep model-learned information at decision level for automated classification of lung nodules on chest CT," Inf. Fusion **42**, 102–110 (2018).
88. B.-C. Kim, J.-S. Choi, and H.-I. Suk, "Multi-Scale Gradual Integration CNN for False Positive Reduction in Pulmonary Nodule Detection," arXiv preprint arXiv:1807.10581 (2018).
89. Y. Qin, et al, "Simultaneous Accurate Detection of Pulmonary Nodules and False Positive Reduction Using 3D CNNs," in 2018 IEEE Int. Conf. Acoust. Speech Signal Process.(IEEE, 2018), pp. 1005–1009.

90. H. Xie, et al., Automated pulmonary nodule detection in CT images using deep convolutional neural networks, Pattern Recognit. **85**, 109–119 (2019).

91. M. Bergtholdt, R. Wiemker, and T. Klinder, "Pulmonary nodule detection using a cascaded SVM classifier," in edited by G.D. Tourassi and S.G. Armato (International Society for Optics and Photonics, 2016), p. 978513.

92. R. Opfer and R. Wiemker, "Performance analysis for computer-aided lung nodule detection on LIDC data," Proc. SPIE **6515**, 65151C–65151C–9 (2007).

93. B. Sahiner et al., "Effect of CAD on radiologists' detection of lung nodules on thoracic CT scans: analysis of an observer performance study by nodule size.," Acad. Radiol. **16**(12), 1518–30 (2009).

94. K. Suzuki, et al., "Massive training artificial neural network (MTANN) for reduction of false positives in computerized detection of lung nodules in low-dose computed tomography," Med. Phys. **30**(7), 1602–1617 (2003).

95. E. Lopez Torres, et al., "Large scale validation of the M5L lung CAD on heterogeneous CT datasets," Med. Phys. **42**(4), 1477–1489 (2015).

96. Q. Dou, et al., "Multilevel Contextual 3-D CNNs for False Positive Reduction in Pulmonary Nodule Detection," IEEE Trans. Biomed. Eng. **64**(7), 1558–1567 (2017).

97. H. Jiang, et al., "An Automatic Detection System of Lung Nodule Based on Multigroup Patch-Based Deep Learning Network," IEEE J. Biomed. Heal. Informatics **22**(4), 1227–1237 (2018).

98. H. Jin, et al., "A deep 3D residual CNN for false-positive reduction in pulmonary nodule detection," Med. Phys. **45**(5), 2097–2107 (2018).

99. Q. Dou, et al., "Automated Pulmonary Nodule Detection via 3D ConvNets with Online Sample Filtering and Hybrid-Loss Residual Learning," in (Springer, Cham, 2017), pp. 630–638.

100. S.A. Patil and V.R. Udupi, "Geometrical and texture features estimation of lung cancer and TB images using chest X-ray database," Int. J. Biomed. Eng. Technol. **6**(1), 58 (2011).

101. S. Aravind Kumar, et al., "Robust and Automated Lung Nodule Diagnosis from CT Images Based on Fuzzy Systems," in 2011 Int. Conf. Process Autom. Control Comput.(IEEE, 2011), pp. 1–6.

102.F. Zhang, et al., “Overlapping node discovery for improving classification of lung nodules,” Annu. Int. Conf. IEEE Eng. Med. Biol. Soc **2013**, 5461–5464 (2013).

Furqan Shaukat is currently working as an Assistant Professor in Department of Electronics Engineering UET Taxila Sub Campus Chakwal. He completed his BSc in Electrical Engineering from UET Lahore in 2007. He received his MSc and PhD degrees from UET Taxila in 2011 and 2018 respectively. He has also worked as Research Associate in University of Sheffield UK during his PhD. His research interests include medical image analysis and classification.

Gulistan Raja received his B.Sc. Electrical Engineering Degree from UET Taxila in 1996. He completed Masters in Information Systems Engineering from Osaka University, Osaka, Japan in 2002 and PhD in Electrical Engineering from UET Taxila in 2008. He is currently serving as Professor of Electrical Engineering at UET Taxila. He has authored/co-authored >90 research publications in reputed international journals and refereed conferences. His research interests include digital image/video signal processing and VLSI design.

Dr. Frangi is Diamond Jubilee Chair in Computational Medicine at the University of Leeds, Leeds, UK, with joint appointments at the School of Computing and the School of Medicine. He has been awarded a Chair in Emerging Technologies by the Royal Academy of Engineering. He leads the CISTIB Center for Computational Imaging and Simulation Technologies in Biomedicine. His main research interests are in medical image computing, medical imaging, and image-based computational physiology.

Caption List

Fig. 1 Samples of lung nodule types. From left to right, well-circumscribed/sloid, juxta-vascular/subsolid, juxta-pleural, pleural-tail and GGO nodules

Fig. 2 Typical lung CAD processes: image acquisition, segmentation of lung fields, detection of candiate nodules, and false positive reduction

Table 1 Public Databases for assessments of Lung CAD_e Systems, *N/A, Not available

Table 2. Review of Lung Segmentation Techniques

Table 3. Review of Lung Nodule Detection Methods

Table 4. Performance Comparison of Different CAD Systems; *N/A, Not available.